INFECTION AND IMMUNITY, Mar. 2005, p. 1441–1451 Vol. 73, No. 3
0019-9567/05/$08.00+0 doi:10.1128/IAI.73.3.1441–1451.2005

Citrobacter rodentium lifA/efa1 Is Essential for Colonic Colonization and Crypt Cell Hyperplasia In Vivo

Jan-Michael A. Klapproth,[1]* Maiko Sasaki,[1] Melanie Sherman,[2] Brian Babbin,[2] Michael S. Donnenberg,[3] Paula J. Fernandes,[3] Isabel C. A. Scaletsky,[4] Daniel Kalman,[2] Asma Nusrat,[2] and Ifor R. Williams[2]

Division of Digestive Diseases[1] and Department of Pathology,[2] Emory University, Atlanta, Georgia; Division of Infectious Diseases, University of Maryland, Baltimore, Maryland[3]; and Departamento de Microbiologia, Imunologia, e Parasitologia, Universidade Federal de São Paulo, São Paulo, Brazil[4]

Received 19 August 2004/Returned for modification 24 September 2004/Accepted 4 November 2004

Previously, we have identified a large gene (*lifA*, for lymphocyte inhibitory factor A) in enteropathogenic *Escherichia coli* (EPEC) encoding a protein termed lymphostatin that suppresses cytokine expression in vitro. This protein also functions as an adhesion factor for enterohemorrhagic *E. coli* (EHEC) and Shiga toxin-producing *E. coli* and is alternatively known as *efa1* (EHEC factor for adherence 1). The *lifA/efa1* gene is also present in *Citrobacter rodentium*, an enteric pathogen that causes a disease termed transmissible murine colonic hyperplasia (TMCH), which induces colitis and massive crypt cell proliferation, in mice. To determine if *lifA/efa1* is required for *C. rodentium*-induced colonic pathology in vivo, three in-frame mutations were generated, disrupting the glycosyltransferase (GlM12) and protease (PrMC31) motifs and a domain in between that does not encode any known activity (EID3). In contrast to infection with wild-type *C. rodentium*, that with any of the *lifA/efa1* mutant strains did not induce weight loss or TMCH. Enteric infection with motif mutants GlM12 and PrM31 resulted in significantly reduced colonization counts during the entire 20-day course of infection. In contrast, EID3 was indistinguishable from the wild type during the initial colonic colonization, but cleared rapidly after day 8 of the infection. The colonic epithelium of all infected mice displayed increased epithelial regeneration. However, significantly increased regeneration was observed by day 20 only in mice infected with the wild-type in comparison to those infected with *lifA/efa1* mutant EID3. In summary, *lifA/efa1* is a critical gene outside the locus for enterocyte effacement that regulates bacterial colonization, crypt cell proliferation, and epithelial cell regeneration.

Citrobacter rodentium is a gram-negative bacterium that colonizes predominantly the distal colon of mice, causing a disease termed transmissible murine colonic hyperplasia (TMCH), which induces colitis and crypt cell proliferation (24). Colonic pathology in infected animals is characterized by massive proliferation of crypt cells, goblet cell depletion, epithelial cell disruption, and mucosal thickening from inflammation. Infected mice lose weight and develop ruffled fur and soft fecal pellets, but usually do not have diarrhea. Depending on the genetic background of the animals, mice clear the infection within 4 weeks and recover completely by week 6.

C. rodentium belongs to a family of enteric gram-negative bacteria that cause attaching and effacing (A/E) lesions characterized by the accumulation of filamentous actin beneath the site of bacterial attachment and loss of microvilli (34). Additional members of this family are enteropathogenic *Escherichia coli* (EPEC) (27) and enterohemorrhagic *E. coli* (EHEC) (13). EPEC and EHEC strains are important causative agents of diarrheal diseases in humans worldwide. EPEC is responsible for infantile diarrhea predominantly in developing countries (28), whereas EHEC causes hemorrhagic colitis which can be complicated by systemic manifestations, such as hemolytic-uremic syndrome (35). Genes encoding the A/E phenotype are located on a large (~35-kb) chromosomal pathogenicity island termed the locus of enterocyte effacement (LEE), which has been associated with the ability to induce diarrheal disease (12, 26, 30). This pathogenicity island contains approximately 41 genes organized into several polycistronic operons (10). Approximately half of the genes located in the LEE encode a type III secretion system that transfers proteins to host cells. Among these genes are those that code for the translocation proteins EspA (19), EspB (30), and EspD (22), which are critical in the pathogenesis of infection in vitro and in vivo. Two additional proteins which are encoded by the LEE and are essential for colonization and induction of an immune response are the outer membrane adhesion molecule intimin and its cognate receptor Tir (translocated intimin receptor). Intimin (15) and Tir (11) in particular appear to be of critical importance for the development of TMCH. Previously, it has been shown that transformation of the LEE pathogenicity island alone into laboratory strains is sufficient to trigger the characteristic A/E lesions in vitro (26).

Beside the LEE pathogenicity island, additional genes outside this well-defined chromosomal region contribute to the pathophysiology of enteric gram-negative infection. Previously, we and others have identified an inhibitory protein named lymphostatin (21) in bacterial lysates from A/E pathogens. Lymphostatin is encoded by a large chromosomal gene, termed *lifA* for lymphocyte inhibitory factor A, in EPEC strain E2348/69. Lymphostatin induces a profound suppression of lymphocyte activation in vitro. Lymphocyte cultures from different

* Corresponding author. Mailing address: Division of Digestive Diseases, Suite 201, Whitehead Biomedical Research Building, Emory University, 615 Michael St., Atlanta, GA 30345-2173. Phone: (404) 727-5638. Fax: (404) 727-5767. E-mail: jklappr@emory.edu.

TABLE 1. Bacterial strains and plasmids used in this study

Strain or plasmid	Description	Source or reference
EPEC E2348/69	O126:H6 isolate from infant diarrhea	22a
C. rodentium	Wild type causing and TMCH and colitis	ATCC
pKD46	Red recombinase system	7
pKD4	PCR template for Km cassette and FRT	7
pFT-A	Helper plasmid encoding for recombinase	32a
p3-B-8	*C. rodentium lifA/efal* cosmid clone	This study
*Cr*pKD46	*C. rodentium* wild type transformed with pKD46	This study
EIB2K1	Kanamycin insertion mutation at bp position 3,496	This study
EID3	Kanamycin-cured *lifA/efa1* non-motif mutant	This study
EI3B8	EID3 complemented *lifA/efa1* on plasmid p3-B-8	This study
G1M9	Kanamycin insertion mutation at bp position 1,672	This study
G1M12	Kanamycin-cured *lifA/efa1* glycosyltransferase motif mutant	This study
PrMC1	Kanamycin insertion mutation at bp position 3,456	This study
PrMC31	Kanamycin-cured *lifA/efa1* protease motif mutant	This study

species preincubated with lymphostatin are unable to produce significant amounts of interleukin 2 (IL-2), IL-4, and gamma interferon protein and do not proliferate in response to mitogen stimulation (20). Interestingly, *lifA* has also been identified to function as an adhesion factor for EHEC E45035N (31) and EPEC JPN 15 (39) and has therefore been termed *efa1* (EHEC factor for adherence). Studies performed in vitro revealed that mutation of E45035N *lifA/efa1* significantly decreased bacterial adherence to cultured epithelial cells.

Cross hybridization experiments and assays for inhibitory activity have identified *lifA/efa1*-similar genes in other gram-negative bacteria that demonstrate the A/E phenotype, including rabbit enteropathogenic *E. coli* 1 (RDEC-1) (44) and mouse pathogen *C. rodentium* (unpublished data). As the study of A/E pathogens in humans is difficult, infection of mice with *C. rodentium* has been used as a surrogate model for human infection with EHEC and EPEC.

Additional genes located outside the LEE pathogenicity island have been identified as critical virulence factors in *C. rodentium* pathogenesis. NleA (non-LEE-encoded effector A) (14) is translocated by the TTSS, targeting the Golgi apparatus for an effect that is currently unclear. Our study was conducted to further clarify the role of *lifA/efa1*, which is not part of the LEE, and its gene product lymphostatin/Efa1 in the pathogenesis of TMCH in mice in vivo. In comparison to animals infected with the wild type, mice infected with mutant *lifA/efa1* strains did not display systemic signs of infection. Infection with a nonmotif mutated strain did not result in significant differences in colonic colonization until day 8. However, deletion-insertion mutation of two critical motifs in *lifA/efa1* resulted in significantly decreased colonic colonization during all time points of the investigation. TMCH did not develop in any of the animals infected with the *lifA/efa1* mutant strains at any time. This report characterizes an additional bacterial gene located outside the LEE pathogenicity island and its critical role in colonic colonization and the pathogenesis of TMCH.

MATERIALS AND METHODS

Bacterial strains, growth conditions, and lysis. The bacterial strains used in this study are listed in Table 1.

To generate bacterial lysates, bacteria were grown overnight in Luria-Bertani broth supplemented with nalidixic acid (50 μg/ml) for EPEC strain E2348/69 and with ampicillin (25 μg/ml) for the *C. rodentium* wild type, EID3, and EI3B8. Bacterial cultures were centrifuged at 4,000 × *g*, washed in phosphate-buffered saline (PBS) once, and lysed by French press at 20,000 lb/in^2. Bacterial cell debris was removed by centrifugation at 1,000 × *g*, and protein concentration was determined by the bicinchoninic acid method (Pierce, Rockford, Ill.).

***C. rodentium* genetic techniques.** Bacterial genomic DNA from *C. rodentium* was partially digested with Sau3AI to yield fragments ranging in size from 20 to 40 kbp and ligated at fivefold molar excess into pHC79 DNA linearized with BamHI. Ligated DNA was packaged by using a commercially available kit (Gigapack II XL; Stratagene, La Jolla, Calif.) and transfected into *E. coli* DH5α grown in LB broth-2% maltose. Transfectants were plated on LB agar supplemented with 50 μg of ampicillin/ml. Individual clones were stored in LB broth-ampicillin (50 μg/ml)-15% glycerol in 96-well plates at −70°C. Screening of the genomic *C. rodentium* library was performed by colony blot hybridization by using a radioactively labeled internal 1.79-kb EcoRI *lifA/efa1* fragment from EPEC E2348/69. Hybridization with an internal *lifA/efa1* EcoRI fragment from EPEC E2348/69 and subsequent restriction digest analysis with EcoRI identified p3-B-8 as the clone with the smallest genomic fragment insertion (approximately 20 kb in size) (data not shown) and expression of inhibitory activity when incubated with activated lymphocyte cultures. p3-B-8 was subjected to commercial shotgun analysis covering the DNA sequence 8 to 10 times with the BigDye Terminator method and the capillary 3700 system (Medigenomix, Martinsried, Germany).

To generate in-frame mutations in the *lifA/efa1* gene, we applied a method described previously (7). An overnight culture of wild-type *C. rodentium* was diluted 1:50 in salt-optimized broth and grown to an optical density at 600 nm (OD_{600}) of 0.6. Bacteria were made electrocompetent and concentrated 200-fold in 10% glycerol-H_2O, and 35 μl was used for transformation with approximately 1 μg of pKD46. Following electroporation (Bio-Rad, Hercules, Calif.) at 2.5 kV, transformed bacteria were recovered in 1 ml of salt-optimized broth with carbon at 30°C for 60 min without antibiotics. Serial dilutions (10^{-4} to 10^{-7}) were plated on LB agar plates containing 200 μg of ampicillin (Sigma Chemical Co., St. Louis, Mo.)/ml and incubated overnight at 30°C. Successful transformation of individual clones was confirmed by adding 3 μl of bacterial culture directly to 45 μl of PCR Supermix HiFi (Invitrogen, Carlsbad, Calif.) and 1 μl of each 20 μM pKD46-specific primer pair for genes encoding Gam (Klapp-110–Klapp-111) and exonuclease protein (Klapp-112–Klapp-113) (Table 2). Reactions were carried out in a Mastercycler (Eppendorf, Hamburg, Germany) with the following program: 94°C for 4 min. followed by 30 cycles of 94°C for 1 min, 53°C for 1 min, and 68°C for 2 min. PCR samples were electrophoresed on a 2% agarose gel, stained in 1% ethidium bromide, and examined under UV light. A single clone containing pKD46 (*Cr*pKD46) was grown in 100 ml of SOB and 10 mM arabinose to an OD_{600} of 0.6, made electrocompetent as outlined above, and stored at −80°C until further use.

In parallel, six *C. rodentium lifA/efa1*-specific primers consisting of 74 to 80 nucleotides each were designed: 54 to 60 nucleotides with *C. rodentium lifA/efa1*-specific sequences and an additional 20 nucleotides recognizing sequences upstream and downstream of the kanamycin resistance cassette in pKD4 (Table 2). Primer pairs were designed not to disrupt the open reading frame (ORF) following recombination with helper plasmid pFT-A (see below). PCR amplification was performed for each primer pair in eight independent reactions consisting of 45 μl of PCR Supermix HiFi (Invitrogen), 10 ng of pKD4 template, and 1 μl of a 20 μM concentration of each primer combination (Klapp-165–Klapp-167, Klapp-102–Klapp-103, and Klapp-169–Klapp-170) (Table 2), utilizing the

TABLE 2. PCR primer combinations for molecular methods

Primer name	Sequence[a]	Description
Klapp-110	5′-ATGGATATTAATACTGAAACTGAG-3′	Gam protein
Klapp-111	5′-TTATACCTCTGAATCAATATCAAC-3′	Gam protein
Klapp-112	5′-ATGACACCGGACATTATCCTGCAG-3′	Exonuclease
Klapp-113	5′-TCATCGCCATTGCTCCCCAAATAC-3′	Exonuclease
Klapp-102	5′-ACAATAAATGGACTAGGGATAACAGGTGTACACACTGCAGAATGCCTGCT ACCGGCACCAgtgtaggctggagctgcttc-3′	bp 3,496–3,555, *lifA/efa1*-pKD4
Klapp-103	5′-CAAATTGTCAAAACCATCAGCAGCACTGACCATCACCTGTTCTGTAATTTT TCCGTTAATcatatgaatatcctccttag-3′	bp 3,640–3,669, *lifA/efa1*-pKD4
Klapp-165	5′-TACTGTATTATGAAGGGAGTTACAGATATTAATGATGAGTTACGAGTAAA CTATgtgtaggctggagctgcttc-3′	bp 1,297–1,350, *lifA/efa1*-pKD4 (glycosyltransferase motif)
Klapp-167	5′-ACGTAGCTTTAAGTCTTCCAGGAAACGATTATCTCCATTTGTTTCCATCAT AATcatatgaatatcctccttag-3′	bp 1,672–1,725, *lifA/efa1*-pKD4 (glycosyltransferase motif)
Klapp-169	5′-CATGCACAGGGATGGTTCGAAGTGGCCAAAGGATATGGCAGCCAGAATA TTGACgtgtaggctggagctgcttc-3′	bp 4,303–4,356, *lifA/efa1*-pKD4 (protease motif)
Klapp-170	5′-TAATTGTATACCAGCCTCAATAAACTTCAGAGCATCCAGGGAAGAAAGGA AATCcatatgaatatcctccttag-3′	bp 4,441–4,494, *lifA/efa1*-pKD4 (protease motif)
Klapp-187	5′-TACTGTATTATGAAGGGAGTTA-3′	bp 1,297–1,318, *lifA/efa1*
Klapp-188	5′-AAGCCCACGTATATTCCATCCG-3′	bp 1,938–1,959, *lifA/efa1*
Klapp-136	5′-AGCAGACGAGTTCAAGGGATA-3′	bp 3,363–3,383, *lifA/efa1*
Klapp-137	5′-CAAATTGTCAAAACCATCAGC-3′	bp 3,649–3,669, *lifA/efa1*
Klapp-201	5′-ATCGTTGAACACGCCAAATAT-3′	bp 4,249–4,269, *lifA/efa1*
Klapp-202	5′-TCTGGTCATCAGGGCATTATC-3′	bp 4,528–4,548, *lifA/efa1*
Klapp-256	5′-AATTCTCATGTTTGACAGCT-3′	pHC79
Klapp-257	5′-AATTCTCATGTTTGACAGCT-3′	pHC79

[a] Uppercase letters, nucleotides with *C. rodentium lifA/efa1*-specific sequences; lowercase letters, nucleotides recognizing sequences upstream and downstream of the kanamycin resistance cassette in pKD4.

PCR program described above. Following amplification, PCRs were pooled, precipitated with isopropanol, dissolved in water, and digested overnight with 10 U of DpnI (New England BioLabs Inc., Beverly, Mass.). Digested PCR fragments were gel purified and dissolved in water, and concentrations were determined at OD_{260} and OD_{280}.

Approximately 1 μg of gel-purified PCR product was electroporated with 2.5 kV into *Cr*pKD46, and transformants were recovered for 2 h in 1 ml of SOC with 10 mM arabinose at 37°C. A 100-μl bacterial culture aliquot was spread on LB agar plates containing 100 μg of kanamycin and incubated at 42°C overnight. Recombinant clones were replica patched on LB agar plates containing ampicillin (200 μg/ml) and kanamycin (100 μg/ml). Mutant clones with a resistance cassette insertion that grew on kanamycin-supplemented but not ampicillin-supplemented plates were confirmed by PCR as described above. Verification of insertion at positions 1,672, 3,496, and 4,303 bp was performed with 1 μl of a 20 μM concentration of each primer in combination (Klapp-187–Klapp-188, Klapp-136–Klapp-137, and Klapp-201–Klapp-202, respectively) (Table 2), utilizing the identical amplification program listed above. Confirmation by PCR led to the identification of insertion mutants EIB2K1 (nonmotif mutant), GlM9 (glycosyltransferase motif mutant), and PrMC1 (protease motif mutant) (Table 1).

To cure the kanamycin resistance cassette from *lifA/efa1*, insertion mutant *C. rodentium* strains EIB2K1, GlM9, and PrM1 were made electrocompetent and transformed as described above, with 100 ng of pFT-A (32). Transformed bacteria were recovered in 1 ml of SOC, spread on LB agar plates with 200 μg of ampicillin/ml, and incubated overnight at 30°C. Recombination of ampicillin-resistant *C. rodentium* containing pFT-A was induced with a 1/10 volume of 200 μg of heat-inactivated chlortetracycline (Sigma)/ml for 6 h at 30°C. Serial dilutions (10^{-4} to 10^{-6}) of bacterial culture were spread on LB agar without antibiotics and recombinant clones were replica patched the following day on three different LB agar plates containing either no antibiotics, ampicillin (200 μg/ml), or kanamycin (100 μg/ml). Individual clones that grew on LB but not on ampicillin- or kanamycin-containing plates were further analyzed by PCR with 1 μl of a 20 μM concentration of each primer in combination (Klapp-187–Klapp-188, Klapp-136–Klapp-137, and Klapp-201–Klapp-202) (Table 2) as outlined above. PCR products from all three mutant strains were gel-purified, cloned into pCR-TOPO2.1 (Invitrogen) according the manufacturer's specifications, and analyzed by sequencing with M13 forward and reverse primers in order to confirm the presence of "scar" sequence and in-frame mutation.

To complement the *lifA/efa1* mutation, EID3 was made electrocompetent and transformed with 1 μg of p3-B-8. Transformed EID3 was selected on LB agar with ampicillin (200 μg/ml) and confirmed by PCR with *lifA/efa1*-specific primer pair Klapp-136–Klapp-137 and a primer combination for vector-specific sequences (Klapp-256–Klapp-257), utilizing the identical PCR protocol outlined above.

PBMC stimulation and lymphokine analysis by enzyme-linked immunosorbent assay (ELISA). Peripheral blood mononuclear cells (PBMC) were isolated from peripheral blood from healthy volunteers. Whole blood was diluted 1:1 in PBS, layered over Histopaque 1077 (Sigma), and centrifuged at 400 × *g* for 20 min at 94°C. Mononuclear cells were aspirated, washed in PBS, and centrifuged at 200 × *g* for 10 min at 23°C. Cell pellets were resuspended in complete RPMI 1640 (Gibco BRL Inc, Grand Island, N.Y.) with 2 mM glutamine, 1 mM sodium pyruvate, 20 mM HEPES buffer (pH 7.4), and 10% heat-inactivated fetal calf serum (Sigma). PBMC were diluted to a concentration of 10^6/ml and incubated at 37°C in a 5% CO_2 atmosphere.

Analysis of lymphokine expression was performed by incubating 10^6 PBMC/ml with increasing concentrations of bacterial lysates, ranging from 2.5 to 50 μg/ml. Following a 2-h preincubation, PBMC cultures were stimulated with a combination of pokeweed mitogen (10 μg/ml) and phorbol myristate acetate (10 ng/ml) as previously described (20). The cell supernatant was analyzed for IL-2 by ELISA (Biosource International, Camarillo, Calif.) according the manufacturer's specifications after a total of 24 h of incubation. Microtiter plates were read at 450 and 650 nm, and the cytokine concentrations in the supernatant were determined with a linear-linear standard curve. Mean values of raw cytokine concentrations were normalized and expressed as percentages of the positive control according the following formula: $(S - N)/(P - N) \times 100\%$ (S, cytokine concentration; P, positive control; N, negative control). Mean values of duplicate cytokine samples from three independent experiments were analyzed by Student's t test, and two-tailed P values of ≤0.05 were considered statistically significant.

Immunofluorescence labeling and confocal microscopy. 3T3 cells were seeded in eight-well chamber slides in Dulbecco's modified Eagle medium (Gibco BRL) and 10% fetal calf serum (Sigma) the day prior to the experiment. Bacterial strains were grown overnight at 37°C without shaking in LB broth (Sigma) supplemented with 50 μg of nalidixic acid/ml (EPEC), 25 μg of ampicillin/ml (*C. rodentium*, EID3), and 100 μg of ampicillin/ml (EI3B8). 3T3 cells were directly infected with 10 μl of EPEC and 50 μl of each *C. rodentium* strain for 5 h. At 5 h, fibroblasts were rinsed three times in Dulbecco's PBS (DPBS) and fixed in 3.7% paraformaldehyde in DPBS for 20 min. 3T3 cells were then rinsed twice with DPBS and permeabilized with 0.2% Triton X-100 for 20 min and blocked with 1% bovine serum albumin in DPBS, pH 7.4, for 1 h. Filamentous actin was labeled with 6.6 nM Alexa Fluor 488 Phalloidin (Molecular Probes, Eugene,

Oreg.). Nuclear counter staining was performed with 1 μM TO-PRO-3 iodide (642/661) for 10 min, followed by two rinses in DPBS. Stained monolayers were examined with a Zeiss LSM510 laser scanning confocal microscope (Zeiss Microimaging, Thornwood, N.Y.) coupled to a Zeiss 100 M Axiovert.

Fibroblast adhesion assay. Prior to experiments determining the numbers of adherent bacteria, we correlated the OD_{600} with CFU for EPEC and *C. rodentium* strains used in this study. The mean CFU per OD unit for EPEC was determined at 2.39×10^7 and for *C. rodentium* strains at 1.48×10^7. A method to quantify bacterial adherence has been described previously (25). Briefly, 3T3 cells were seeded into 96-well plates the day prior to infection with bacteria. Following the removal of antibiotics by rinsing cells in PBS three times, cultures were inoculated in triplicate with 5×10^6 CFU per strain and per well, centrifuged at $400 \times g$ for 15 min at room temperature, and incubated at 37°C and 5% CO_2 for a maximum of 4 h. Cells were washed three times with PBS for 4 h and lysed with 1% Triton X-100–PBS for 5 min. Serial dilutions were spread on MacConkey agar plates and counted the following day. Data from three independent experiments were calculated as mean CFU with standard errors (SE) per 10^5 3T3 cells and subjected to Student's *t* test for statistical analysis.

Mouse strains and oral infection. Animal use and in vivo research complied with all relevant institutional policies and federal guidelines. Female, 4- to 6-week-old, pathogen-free C57BL/6 mice were purchased from the Jackson Laboratory (Bar Harbor, Maine). Animals were kept in cages, in groups of five animals per cage, with unlimited access to water and food throughout the experiment. Mice used in this study were weighed prior to infection to determine mean baseline weights and every day thereafter. Weight was normalized, and changes were expressed as percent changes in comparison to the baseline.

Bacterial strains were grown overnight in LB medium, centrifuged at $400 \times g$, and washed once in PBS. Following a second centrifugation step, bacterial cultures were resuspended in PBS, and numbers of CFU were approximated by measuring the OD_{600}. Groups of five animals for each time point (days 2, 8, 14, and 20) and the EPEC, *C. rodentium* wild type, EID3, EI3B8, GlM12, and PrM31 groups were orally infected with 100 μl of PBS containing an approximately 3×10^8 CFU bacterial solution per strain; control mice received PBS only. To determine the exact infectious dose per animal, serial dilutions of the bacterial solutions were plated on MacConkey II agar plates (Becton Dickinson and Co., Sparks, Md.), incubated at 37°C overnight, and enumerated the following day.

Tissue collection. Animals were euthanized on days 2, 8, 14, and 20 of the infection by terminal anesthesia with isoflurane (Abbott Laboratories, North Chicago, Ill.) followed by cervical dislocation. The distal colon from each animal was excised from the anal verge to mid-colon and divided into two equal parts of approximately 0.5 cm in length. The proximal section of the distal colon was fixed in formalin solution for histological analysis, and the distal section was homogenized in 1 ml of PBS to determine colon colonization.

Bacterial colonization counts. Following removal of all fecal pellets, the distal section of colon of approximately 0.5 cm in length from each animal was weighed and homogenized in 1 ml of PBS at low speed with a Tissuemizer (Fisher Scientific, Pittsburgh, Pa.). Serial dilutions of tissue homogenate in LB broth were plated on MacConkey agar (Becton Dickinson) plates and enumerated the following day. Only colonies that displayed the characteristic pink center surrounded by a white rim (*C. rodentium* strains) or a purely pink appearance (EPEC E2348/69) were counted. Colon colonization was calculated and expressed as CFU per gram of tissue with standard errors. Statistical analysis was performed by utilizing the Mann-Whitney U test ($P \leq 0.05$).

Transmission electron microscopy. Colonic tissue from control and infected mice was fixed in 4% glutaraldehyde and cut into 1-μm strips by using a microtome. The strips were postfixed in 1% osmium tetroxide, sequentially dehydrated through graded alcohols and propylene oxide, and then infiltrated with Embed-812 (Electron Microscopy Sciences, Ft. Washington, Pa.). Strips were embedded for cross-section orientation. Semithin (0.5-mm) sections were cut, stained with toluidine blue, and examined for adequacy. Ultrathin (900-Å) sections were cut with a diamond knife, stained with uranyl acetate and lead citrate, and examined with an EM201 electron microscope (Philips Electronics, Mahawah, N.J.).

Histology. Following removal of the distal colon from each animal used in this study, the proximal section of distal colon was fixed in a 10% (vol/vol) formalin solution for 2 days and processed for embedding in paraffin. Transverse sections (5 μm) were stained with hematoxylin and eosin. Histological analysis was performed by two independent pathologists who were blinded to the experimental conditions. Tissue sections from infected and uninfected mice in all groups were analyzed on day 2, 8, 14, and 20 for epithelial regenerative changes and the nature of the inflammatory cell infiltrate. Regenerative changes were identified based on cytological changes of crypt epithelial cells and mucosal thickness. The cytological criteria used were increased nuclear-to-cytoplasmic ratio, increased mitotic activity, and diminished mucin production. Mucosa from control animals was used to define baseline mucosal thickness. Alterations in thickness are expressed as a percent increase from the baseline. Cytological changes were graded as 1+ (no changes), 2+ (minimal, involving crypts with ≤20% increases in mucosal thickness), 3+ (mild, extending up to half of the crypt height with 20 to 80% increases in mucosal thickness), 4+ (moderate, extending over half of the crypt height with surface maturation and with 80 to 100% increases in mucosal thickness), and 5+ (florid, involving the entire crypt and surface epithelium with >100% increases in mucosal thickness). Scores determined for epithelial regenerative changes were analyzed by Student's *t* test ($P \leq 0.05$).

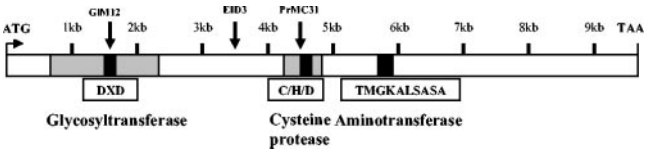

FIG. 1. The *C. rodentium lifA/efa1* gene. The *lifA/efa1* gene from *C. rodentium* was identified on cosmid clone p3-B-8 by testing bacterial lysates in an inhibitory assay and cross hybridization with an internal EcoRI fragment from EPEC strain E2348/69 *lifA/efa1*. The D-X-D motif in *C. rodentium lifA/efa1*, encoding a glycosyltransferase activity and inactivating small GTP-binding proteins, is also present in large clostridial cytotoxins. The protease motif is present in avirulence proteins of plant pathogens and YopT, and it disrupts the actin cytoskeleton in host cells. The third distinct motif present in *C. rodentium lifA/efa1* encodes an aminotransferase II. Areas in grey indicate domains with significant sequence similarities to known motifs present in other gram-negative bacteria. Three domains of the *lifA/efa1* gene in *C. rodentium* were mutated, generating mutant GlM12, PrMC31, and EID3 (arrows).

Statistical analysis. Nonparametric analysis of organ colonization counts was performed by Mann-Whitney U test. Data from IL-2 suppression, bacterial fibroblast adhesion, weight changes, and epithelial regenerative changes were subjected to Student's *t* test. Differences were considered significant if *P* was ≤0.05.

Nucleotide sequence accession number. The nucleotide sequence of *C. rodentium lifA/efa1* is available at GenBank under accession number AY726731.

RESULTS

Identification and sequence analysis of *lifA/efa1* of *C. rodentium*. The cosmid clone p3-B-8 generated from *C. rodentium* serotype 4280 contained a single large ORF (Fig. 1) that was 9,627 bp in size and encoded a protein with a calculated size of 363,588 Da. The G/C content of this ORF was 42%, which is lower than that of the genomic DNA from K-12 *E. coli*. A protein-protein BLAST search including the entire length of translated *C. rodentium lifA/efa1* sequence identified significant similarities for *lifA/efa1* from EPEC E2348/69 (85%, 9,669 bp, 365,968 Da), which was slightly larger in size. Additional similarities were identified for *lifA/efa1* from EHEC strains O157:H^- (85%), O157:H7 (68%), and RIMD 0509952, as well as for genes present in two obligate intracellular pathogens, *Chlamydophila caviae* (*Chlamydia psittaci*) (33) and *Chlamydia muridarum*. Interestingly, *C. muridarum* harbors two tandem *lifA/efa1* homologous sequences separated by only 21 bp. Analogous to *lifA/efa1* in EPEC, *C. rodentium lifA/efa1* encodes three distinct motifs: glycosyltransferase motif at amino acid positions 553 to 555, a protease motif with three critical residues at 1,466, 1,568, and 1,584, and an aminotransferase II motif from amino acids 1,932 to 1,941.

Limiting the sequence analysis to approximately 500 amino acids flanking the glycosyltransferase motif, additional significant similarities were identified, as previously reported, for the

N-terminal residues of large clostridial cytotoxins. These include α toxin from *Clostridium novyi* (4), toxins A and B from *Clostridium difficile* (18), and lethal toxin from *Clostridium sordellii* (3, 17). Relevant sequence similarities coding for a glycosyltransferase motif were also identified for *Chlamydia trachomatis* and various *Plasmodium* spp., including *P. falciparum*, *P. vivax*, and *P. yoeleii*. The second distinct motif in *C. rodentium lifA/efa1* is located at residues 1,466, 1,568, and 1,584 and encodes a cysteine protease motif. This protease motif consists of three conserved amino acids that have been shown to be of equal importance for biological activity, including a cysteine, histidine, and aspartic acid residue, respectively. The motif is present in a number of other bacterial proteins and has been well characterized for YopT (*Yersinia* outer membrane protein T). YopT cleaves posttranslationally prenylated Rho GTPases (38), resulting in disruption of the cellular actin cytoskeleton (37). A third conserved region, from amino acids 1,932 to 1,941, codes for an aminotransferase II motif. It consists of 10 residues, TMGKALSASA, which are present in other pyridoxal phosphate-dependent enzymes, covalently binding pyridoxal phosphate to a lysine residue.

***lifA/efa1* mutations in *C. rodentium* and complementation.** To characterize the role of *lifA/efa1* in vivo, we generated three insertion-deletion mutations at bp positions 1,350, 3,556, and 4,356 (Fig. 1). Mutations at 1,350 and 4,356 bp were chosen to inactivate the glycosyltransferase and protease motif, deleting amino acids 451 to 557 and 1,453 to 1,480, respectively. The third location for a mutation at 3,556 bp was generated to delete amino acids 1,186 to 1,256 of the protein, thereby leaving known motifs intact. Activation of pKD46 in wild-type *C. rodentium* resulted in recombination of linear PCR products containing the kanamycin resistance cassette into wild-type *lifA/efa1*, generating strains EIB2K1, GlM9, and PrMC1, increasing the size of the *lifA/efa1* gene by 1,477 bp. The kanamycin resistance cassette was cured by utilizing helper plasmid pFT-A. As expected, deletion of the resistance cassette decreased *lifA/efa1* by 129 bp in position 3,355 bp, by 237 bp in position 1, and by 350 bp and no net loss in position 4,356 bp (data not shown). To determine if the scar sequence, consisting of a single FLP recognition site, was in frame with the remainder of the *lifA/efa1* ORF, all mutated *lifA/efa1* sequences were cloned and sequenced in the 5′ and 3′ directions. Sequence analysis confirmed that additional, accidentally introduced nucleotides were absent and that the 84-bp scar sequence was in frame with the *lifA/efa1* ORF for all three mutants (data not shown).

Plasmid p3-B-8 containing *lifA/efa1* was used to complement *lifA/efa1* mutant *C. rodentium* strain EID3 (see above). Following electroporation and selection, individual colonies were subjected to PCR analysis, confirming the presence of vector and wild-type *lifA/efa1* sequences.

In vitro analysis of lysates from EPEC, *C. rodentium*, EID3, and EI3B8 for IL-2 suppressive activity. Previously, we have characterized *lifA/efa1* to code for a lymphokine-inhibitory activity leading to profound suppression of IL-2 expression in vitro. Analogous to these experiments, we lysed wild-type EPEC strain *E2348/69* and *C. rodentium*, as well as mutant clones EID3 and complemented strain EI3B8 by French press. As expected, lysates from wild-type E2348/69 and *C. rodentium* led to dose-dependent suppression of IL-2 protein expression after 24 h of culture (Fig. 2A). In comparison to wild-type *C. rodentium* and EI3B8, lysates from *lifA/efa1* mutant strain EID3 did not contain significant inhibitory activity at concentrations equal to or greater than 5 μg/ml (Student's *t* test, $P \leq 0.05$).

Fibroblast attaching and effacing assay in vitro. EPEC, EHEC, and *C. rodentium* belong to a family of bacteria that upon adhesion to epithelial cells induce the accumulation of filamentous actin beneath the site of bacterial attachment and loss of microvilli, termed A/E. We have shown previously that a mutation in *lifA/efa1* did not interfere with the ability of EPEC strain E2348/69 to induce A/E lesions in Hep-2 cells in vitro (21). However, this mutation was located in the C-terminal portion of *lifA/efa1*, whereas for the present study we introduced a mutation in the N-terminal half of *lifA/efa1*. We therefore sought to determine the effect of an N-terminal mutation on the ability of *C. rodentium* to induce attaching lesions in 3T3 fibroblast cells.

Actin accumulated underneath the site of bacterial attachment was observed for all four strains used in this study (Fig. 2B). Characteristically, EPEC formed clusters of microcolonies, whereas *Citrobacter* strains displayed a more diffuse pattern of adherence over the entire cell surface area. Comparing EPEC and the *C. rodentium* wild type to EID3 and EI3B8, we were unable to detect a difference in quality and quantity of actin pedestal formation after 4 h of infection. Therefore, mutation of *lifA/efa1* did not interfere with the formation of characteristic attaching lesions in 3T3 cells in vitro.

Quantification of bacterial adhesion to 3T3 cell cultures. To quantify the number of cell-associated bacteria, we infected 3T3 cells with 5×10^6 CFU of EPEC, *C. rodentium*, EID3, or EI3B8. As expected, the numbers of adherent bacteria increased over time when measured at 4 h postinfection for all four strains investigated. We did not observe a statistically significant difference comparing the numbers of adherent bacteria to 3T3 cells at 4 h after infection with *C. rodentium* wild type, EID3, and EI3B8 strains (Fig. 2C), as determined by Student's *t* test. Therefore, bacterial adherence to 3T3 fibroblasts was independent of *lifA/efa1* in vitro.

Weight loss during *C. rodentium* infection. To determine the systemic effect of *lifA/efa*1 in vivo, we infected female 4- to 6-week-old C57BL/6 mice by gavage with EPEC, the *C. rodentium* wild type, *lifA/efa1* mutant EID3, and complemented mutant EI3B8. EPEC functioned as a negative control, as it poorly colonizes mouse intestine and induces only minimal pathological changes. Animals were weighed prior to infection and every day thereafter throughout the 20-day experiment. Body weights were expressed as percent changes in comparison to the baseline at day 0 (Fig. 3).

In contrast to mice infected with wild-type *C. rodentium*, animals inoculated with mutant *lifA/efa1* strain EID3 steadily gained weight throughout the experiment. Growth curve shape and overall increase in mean body weight of the EID3 group were identical to those of EPEC-infected and uninfected control mice. These mice steadily gained weight to 110% of baseline by day 20. Stool samples examined from these animals were never loose, nor did these animals exhibit decreased activity or perianal fecal staining. As expected, all mice infected with wild-type *C. rodentium* started to lose weight by day 5, and this weight loss continued until day 13 of the infection,

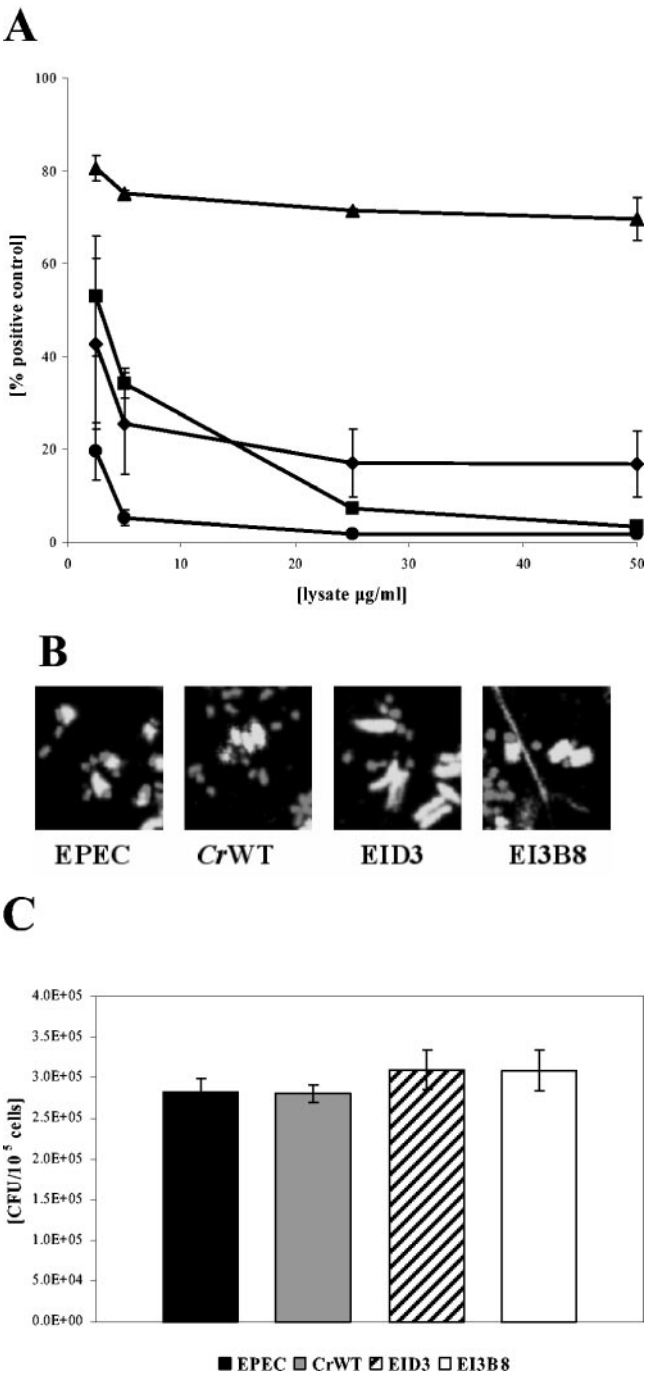

FIG. 2. (A) Bacterial lysates from *lifA/efa1* mutant strain EID3 lose IL-2 inhibitory activity. PBMC (10^6/ml) were preincubated for 2 h with increasing concentrations (ranging from 2.5 to 50 μg/ml) of bacterial lysates from EPEC (♦), *C. rodentium* wild type (■), *lifA/efa1* mutant strain EID3 (▲), and complemented mutant EI3B8 (●). Lymphocyte cultures were activated with the combination of pokeweed mitogen (10 μg/ml) and phorbol myristate acetate (10 ng/ml). After a total of 24 h of incubation, supernatants were aspirated and analyzed in duplicate by ELISA. Data from three independent experiments were pooled, and mean values with SE normalized against values for the positive control were set at 100%. Unlike lysates from generated from EPEC, *C. rodentium*, and EI3B8, lysates from *lifA/efa1* mutant EID3 failed to inhibit expression of IL-2 protein in activated lymphocyte cultures. This difference was statistically significant ($P < 0.05$) at concentrations of 5 μg/ml and greater for *C. rodentium* EI3B8 than for lysates from EID3. Statistical differences were determined by Student's *t* test and considered significant if P was ≤ 0.05. (B) Formation of attaching lesions in 3T3 cells in response to infection with EPEC, C. *rodentium* (*Cr*WT), EID3, and EI3B8. 3T3 cell cultures were infected with EPEC, *C. rodentium*, EID3, and EI3B8 for 5 h, rinsed in PBS, fixed in paraformaldehyde, and stained for nucleic acids and filamentous actin. Images were obtained with a Zeiss Axiscope and digital imaging package. The accumulation of filamentous actin underneath the site of bacterial adherence was not affected by a mutation in *lifA/efa1*, as mutant and wild-type bacteria induced similar attaching lesions in 3T3 fibroblast cultures. (C) Quantification of bacterial adherence to fibroblast cultures. 3T3 cells were infected with 5×10^4 CFU of wild-type EPEC and *C. rodentium* (CrWT), *lifA/efa1* mutant EID3, and complemented strain EI3B8. Infection was allowed to proceed for 4 h, when cell cultures were washed three times with PBS and lysed in 1% Triton X-100. Serial dilutions were plated on MacConkey agar plates, incubated overnight, and enumerated the following morning. Bacterial adherence to fibroblast cells was determined in triplicate in three independent experiments. Data are expressed as means, with error bars representing SE of the means, and were subjected to Student's *t* test for statistical analysis ($P \leq 0.05$). Regardless of the presence or absence of an intact *lifA/efa1* gene, wild-type and mutant *C. rodentium* adhered with equal efficiency to fibroblast cultures at 4 h of infection.

after which the animals started to recover rapidly. Mice infected with *C. rodentium* lost, on average, 13% of their body weight by day 13. This group of animals displayed reduced activity, perianal fecal staining, and loose fecal pellets. We observed statistically significant differences (Student's *t* test, $P \leq 0.05$) in weight between days 10 to 16 comparing wild-type *C. rodentium*-infected mice with controls or animals that received mutant strain EID3. Interestingly, groups of animals that received the complemented strain EI3B8 failed to gain weight throughout the experiment and did not exhibit the characteristic decrease in body weight observed for wild-type infected animals. In fact, by day 20, these animals had lost approximately 3% of their baseline weight. In a comparison of complemented mutant strain EI3B8 to *lifA/efa1* mutant EID3, EPEC, and uninfected controls, a significant difference in weight was observed between days 13 and day 20 of infection (Student's *t* test, $P \leq 0.05$). Therefore, *lifA/efa1* mediates systemic manifestations of infection with *C. rodentium*.

Transmission electron microscopy of colonic tissue sections. To verify that the *C. rodentium* strains used in this study formed A/E lesions in vivo, tissue from mice sacrificed on day 8 was subjected to transmission electron microscopy. As shown in Fig. 4, the *C. rodentium* wild type, EID3, and EI3B8 formed the characteristic A/E lesions in vivo in infected mice. However, we were unable to detect A/E lesions in vivo in mice infected with EPEC strain E2348/69, which is consistent with the observation that EPEC usually does not induce disease in laboratory animals. Therefore, mutation of *lifA/efa1* in *C. rodentium* does not interfere with the formation of A/E lesions in vivo.

Colon colonization with EPEC, *C. rodentium*, EID3, and EI3B8. Previous in vivo and in vitro experiments revealed that *lifA/efa1* plays a role in bacterial colonization. Cattle infected with *lifA/efa1* mutant Shiga toxin-producing *E. coli* (STEC) strains displayed a decrease in fecal shedding in comparison to wild-type infection (39). We therefore sought to determine if the observed changes in body weight were due to a decreased ability of *lifA/efa1* mutant *C. rodentium* to colonize the colon of infected mice.

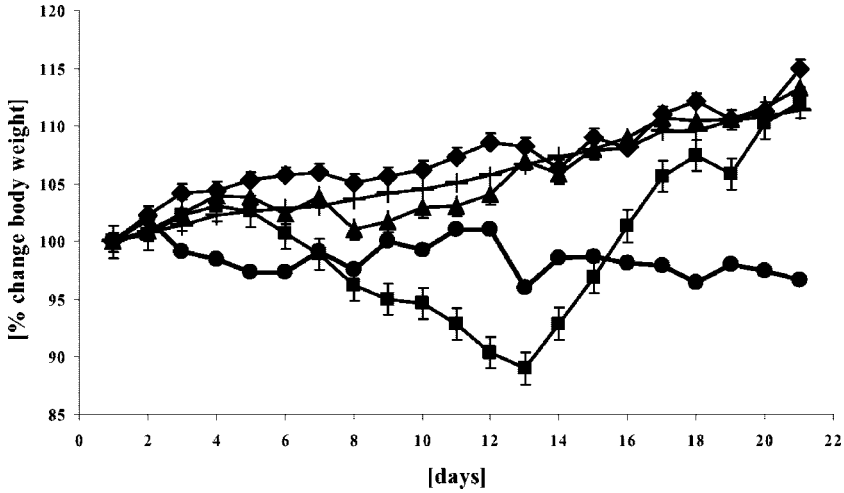

FIG. 3. Weight chart for mice infected with EPEC and *C. rodentium* strains. Enteric infection of groups of five mice with EPEC (♦), *C. rodentium* (■), EID3 (▲), and EI3B8 (●) was initiated by gavage with 3×10^8 CFU/animal in 100 μl of PBS on day 0. Animals were weighed daily until day 20 of infection, and data are expressed as means with error bars for SE. Statistical analysis was performed by Student's *t* test, and results were considered significant if P was ≤0.05. In comparison to mice infected with wild-type *C. rodentium*, EID3 did not induce signs and symptoms of systemic disease, and animals gained weight throughout the 20-day experiment. Weight gain for control mice (○) and animals infected with EID3 and EPEC was indistinguishable.

Colony counts comparing EPEC, *C. rodentium*, EID3, and EI3B8 on day 2 of the experiment did not reveal significant differences (Fig. 5A). By day 8, colonization with *C. rodentium* wild type, EID3, and EI3B8 had increased by approximately 3 log CFU/g of tissue. However, we did detect a significant difference in colonization of approximately 1 log fold comparing wild-type *C. rodentium* to EID3 ($P = 0.032$) on day 8. The *C. rodentium* wild type and EI3B8 were able to maintain a high colonization count in the distal colon on day 14, but EID3 displayed a 4-log-fold reduction in CFU/gram of tissue, counts comparable to those for EPEC. By day 20 of the infection, colonization numbers were comparable for all four strains, without significant differences. Throughout the 20-day experiment, wild-type *C. rodentium* and EI3B8 were indistinguishable in their ability to colonize the colon and we did not identify significant differences at any of the four time points investigated. This result was surprising, as we were unable to detect p3-B-8 or *lifA/efa1* wild-type-specific sequences by PCR in individual bacterial colonies or whole colon homogenates beyond day 2 of infection with EI3B8, indicating that the plasmid was not stable in vivo. As expected, EPEC was rapidly cleared from the colon of infected animals, with the highest bacterial counts occurring on day 2 and persistently low CFU thereafter. Interestingly, mice infected with wild-type *C. rodentium* had significant higher colonization counts in other organs investigated, including mesenteric lymph nodes, liver, small bowel, and spleen (data not shown).

lifA/efa1 encodes a glycosyltransferase and protease motif which have been implicated in the pathogenesis of bacterial infection. In a separate experiment, our goal was to define the role of these two critical motifs in colonic colonization. Time course and infectious dose were identical, as described for Fig. 5A. In this second colonization experiment, wild-type *C. rodentium* was able to maintain high colonization counts beyond day 14, as CFU/gram of tissue were still elevated on day 20 (Fig. 5B). Remarkably, GlM12 and PrM31 were significantly less able to colonize the distal colon than wild-type *C. rodentium* throughout the 20-day experiment. Despite an increase in colony counts for GlM12 and PrMC31, this difference was approximately 1 log fold on days 2 and 8 and increased 2 and 3 log fold by days 14 and 20, respectively.

We conclude that during the initial phase of infection, mu-

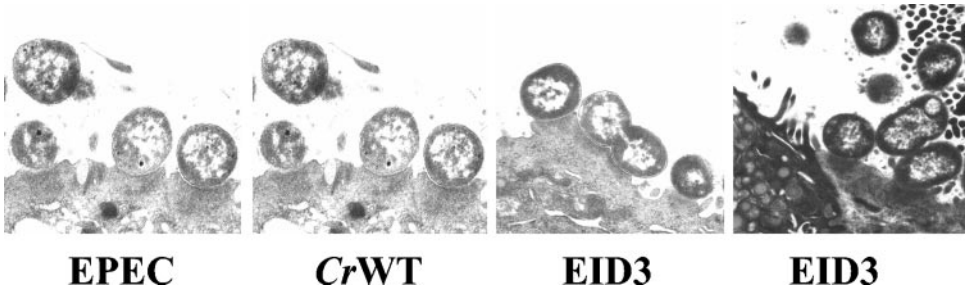

FIG. 4. Transmission electron microscopy of EPEC, *C. rodentium* wild type, EID3, and EI3B8 on day 8 of infection. Morphology of colonic tissue from infected mice at day 8 of infection was evaluated by transmission electron microscopy. Epithelial pedestal-like structures consistent with A/E lesions were observed in the apical pole of epithelial cells infected with *C. rodentium* wild type (*Cr*WT), EID3, and EI3B8.

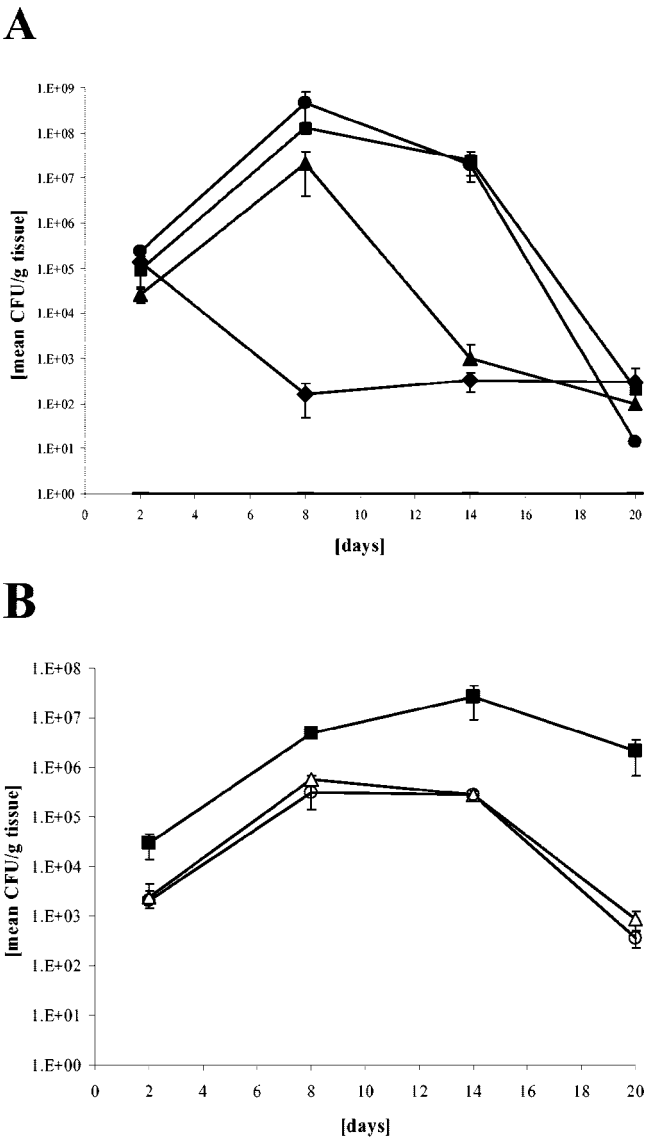

FIG. 5. Bacterial counts of EPEC, *C. rodentium*, EID3, and EI3B8 isolated from the colon of infected mice. Following inoculation with EPEC (♦), *C. rodentium* (■), EID3 (▲), and EI3B8 (●) (A), wild-type *C. rodentium* (■), GlM12 (△), and PrM31 (○) (B) on day 0, animals were sacrificed on day 2, 8, 14, or 20. Fecal pellets were removed from the distal colon of infected animals, and tissue was weighed and homogenized at low speed. Serial dilutions were plated on MacConkey agar, and recovered bacteria were counted the following day. Data depict the mean CFU per gram of colon tissue of infected animals, with bars representing the SE of the mean. Nonparametric analysis of organ colonization counts was performed by the Mann-Whitney U test. (A) Wild-type *C. rodentium* (■) and mutant EID3 (▲) were able to colonize the colon of infected animals with equal efficiency until day 8, after which EID3 was rapidly cleared from the colon, decreasing to levels similar to the CFU determined for EPEC (♦). (B) Mutations in the glycosyltransferase (△) and protease motif (○) resulted in significantly reduced colonic colonization throughout the infection in comparison to wild-type *C. rodentium* infection (■).

tant EID3 was able to colonize the colon of infected mice as efficiently as wild-type bacteria. However, in comparison to wild-type *C. rodentium* and EI3B8, EID3 had an accelerated course of clearance from the colon between day 8 and day 14. In addition, the glycosyltransferase and protease motifs of *lifA*/*efa1* are both equally important for sustained colonic colonization in infected mice.

Epithelial regenerative changes in response to infection with EPEC, *C. rodentium*, EID3, and EI3B8. We next analyzed epithelial regenerative changes from the distal colon of infected animals on day 2, 8, 14, and 20 following inoculation. To quantify regenerative changes observed during the 3-week experiments, two pathologists examined tissue sections from control and experimental mice in a blinded fashion. Epithelial regenerative changes were scored ranging from mild (1+) to florid (5+).

In comparison to uninfected mice, mice infected with wild-type EPEC, wild-type *C. rodentium*, EID3, and EI3B8 all exhibited an increase in epithelial regenerative changes during the course of infection (Fig. 6A). Regenerative changes were observed as early as day 2 in mice infected with EID3. In the same group, markedly increased regenerative scores were recorded for days 8 and 14 and sustained through day 20. There was no significant difference between groups of infected animals on day 8 or 14. However, a significant increase in epithelial cell regeneration was observed on day 20 for animals infected with wild-type *C. rodentium*, the infection being significantly less severe in mice inoculated with EID3 (Fig. 6A). Based on these observations, it appears that lymphostatin/Efa1 is an additional bacterial factor that contributes to epithelial regeneration in mice infected with *C. rodentium*.

Histological changes in response to infection with *C. rodentium* occur as early as 2 days after infection and are fully developed between days 14 and 20. On days 8, 14, and 20, distal colonic sections from mice infected with EPEC, *C. rodentium*, EID3, and EI3B8 were embedded in paraffin and stained with hematoxylin and eosin (Fig. 6B). All infected mice displayed in increase in mucosal thickness, which was in part due to epithelial cell regeneration. Regeneration was still prominent on day 14 and maintained until day 20. As described previously, marked histological changes with inflammation and crypt cell proliferation were apparent in mice infected with wild-type *C. rodentium* by day 8 and continued to progress until the end of the experiment on day 20. Interestingly, mild crypt cell proliferation was also present in the EID3 group, peaking on day 14. By day 20, pathological changes had completely normalized in mice infected with EPEC and EID3. Mucosal thickness doubled in *C. rodentium* wild-type-infected mice in comparison to control and EPEC-infected animals. Interestingly, a mixed inflammatory infiltrate consisting of lymphocytes and neutrophils was observed only with infection with *C. rodentium* wild type on days 14 and 20 and with infection with EI3B8 on day 14.

DISCUSSION

Enteric bacteria face an array of host defense mechanisms that prevent their colonization, multiplication, and invasion. Beside intestinal motility and fluid secretion, the innate and adaptive mucosal immune responses are of critical importance for containment and clearance of infection. However, enteric pathogens have developed strategies that manipulate and counteract immune activation to promote survival of their own species.

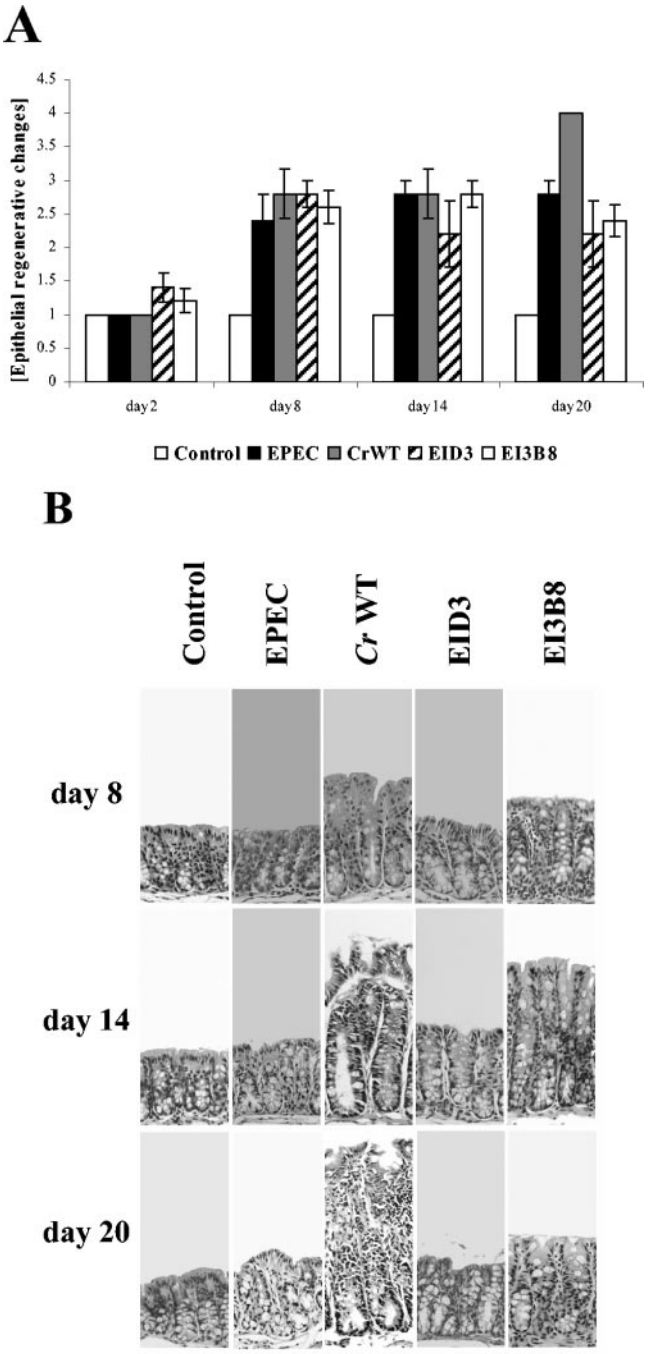

FIG. 6. Time course of epithelial cell regenerative and histological changes in response to infection with EPEC, *C. rodentium*, EID3, and EI3B8. (A) Epithelial regenerative changes for all animals per group were analyzed by two pathologists in a blinded manner on days 2, 8, 14, and 20. The analysis included control animals and mice infected with EPEC, *C. rodentium* (CrWT), EID3, and EI3B8. Cytological changes were graded as 1+ (no changes), 2+ (minimal, involving crypts with ≤20% increases in mucosal thickness), 3+ (mild, extending up to half crypt height with 20 to 80% increases in mucosal thickness), 4+ (moderate, extending over half of crypt height with surface maturation and with 80 to 100% increases in mucosal thickness), and 5+ (florid, involving entire crypt and surface epithelium with >100% increases in mucosal thickness). Scores determined for epithelial regenerative changes were analyzed by Student's *t* test ($P \leq 0.05$). Interestingly, all infected animals responded with increased regenerative scores on days 2, 8, 14, and 20 of infection. A statistically significant difference in regeneration was determined on day 20 of infection in a comparison of scores obtained for EID3 and *C. rodentium* wild type. (B) Distal colonic sections from each animal were fixed in formalin and embedded in paraffin, and transverse 5-μm sections were stained with hematoxylin and eosin. In comparison to control mice inoculated with PBS, all groups responded with increased regenerative scores. TMCH developed only in wild-type *C. rodentium* (*Cr* WT)-infected mice by day 8 and increased in severity by day 20.

In the present study, we have begun to characterize the function of *lifA/efa1* from *C. rodentium* in vivo and its role in colonic colonization, the development of colitis, and crypt cell proliferation.

Lymphostatin/Efa1 has been characterized as an adhesion factor for gram-negative bacteria, including EPEC JPN15 (1) and EHEC strains E45035N (31) and O157:H7 (42). Mutations of *lifA/efa1* in E45035N, O157:H7, and JPN15 or pretreatment with polyclonal antibodies against lymphostatin/Efa1 lead to markedly deficient adherence to epithelial cells when tested in vitro. In addition, inactivation of *lifA/efa1* in STEC serotypes O5 and O111 resulted in a reduced association with cultured HeLa cells (39). In the same study, inoculation of 4- to 11-day-old calves with mutant STEC led to significantly reduced numbers of shed bacteria in the feces, which is currently the only available in vivo data regarding lymphostatin/Efa1. In addition, there is support for a regulatory function of *lifA/efa1* in bacterial adherence as lymphostatin/Efa1 appears to regulate certain bacterial factors that are important for adhesion (42). These factors include *espA*, *espB*, and intimin, which were significantly decreased in bacterial lysates from *lifA/efa1* mutant O157:H7.

In contrast, our previous and present findings (Fig. 2 and 4) suggest that mutant and wild-type *lifA/efa1* strains display differences in colonization but are equally efficient in adhering to epithelial cells by establishing attaching lesions in vitro and in vivo. This difference might be explained by the fact that certain gram-negative bacteria rely on additional factors that mediate adhesion to receptors on the cell surface. Unlike EHEC strains, EPEC E2348/69 and *C. rodentium* harbor a mechanism that potentially mediates bacterial adherence to epithelial cells, the type IV pilus. In EPEC strains, the bundle-forming type IV pilus is found on a 50- to 70-MDa plasmid (40), whereas in *C. rodentium* the pilus-encoding sequence is located on the bacterial chromosome (29). Signature-tagged mutagenesis of *C. rodentium* identified a novel type IV pilus gene cluster that is required for colonization in vivo with similarity to genes from enterotoxigenic *E. coli* and *Vibrio cholerae*. However, in contrast to results of experiments performed with cattle, we did not find a role for lymphostatin/Efa1 as an adhesion molecule in infected rodents. In the study by Mundy et al., a mutation 736 bp downstream from *C. rodentium lifA/efa1*, but not *lifA/efa1* itself, resulted in an insignificant effect on bacterial virulence in vivo with normal colonization between days 2 and 5. It is interesting that in the nonmotif mutant EID3, a significant difference in colonization in comparison to wild-type *C. rodentium* was not observed until day 8 of infection (Fig. 5A). These in vivo findings in mice are consistent with our observations that *lifA/efa1* is not a primary adhesion molecule. First, we did not measure a statistically significant

difference in adherence to 3T3 fibroblast cultures in vitro comparing wild-type and mutant *lifA/efa1 C. rodentium* strains. Second, a mutation in *lifA/efa1* did not affect colonization of EID3 until day 8 of infection. The third argument against lymphostatin/Efa1 as a primary adhesion molecule is the fact that the *C. rodentium* wild type, EID3, and complemented mutant EI3B8 all induced A/E lesions on day 8 of infection. Fourth, colonization counts for wild-type *C. rodentium* and EI3B8 were indistinguishable at every time point during the entire course of infection, despite the fact that we were unable to detect *lifA/efa1* wild-type gene- or vector-specific sequences by PCR beyond day 2 of the infection with EI3B8. This phenomenon is not unexpected, as wild-type bacteria poorly retain cloned DNA and lose plasmids if selective pressure is not maintained with antibiotics. However, these findings allow for the argument that additional early events other than bacterial adhesion play a significant role in successful colonization of *C. rodentium*. It is currently unclear which early events are involved, but we speculate that besides exhibiting an effect on the adaptive immune response, *lifA/efa1* might be involved in modulation of the innate immunity.

Components of the innate immunity encompass phagocytes, epithelial cells, NK cells, and the complement system. It is conceivable that *lifA/efa1* exhibits a positive or inhibitory effect on innate immunity by regulating cytokine expression and phagocytosis, as has been described for EPEC. EPEC induces IL-8 expression in epithelial cell cultures by activating the mitogen-activated protein kinase pathway (6) and prevents its own phagocytosis by inhibition of phosphatidylinositol 3-kinase-dependent pathways (5). It is also possible that *lifA/efa1*-induced modulation of the innate immunity results in a decreased adaptive immune response, allowing for high colonization counts in *C. rodentium* wild-type-infected mice on day 8 and 14. Possible linking mediators involved include cationic peptides, such as LL-37 (8) or defensins (41, 43), which function as immune adjuvants and are found in abundance in inflamed tissue. In this context, it is tempting to speculate that a *lifA/efa1*-induced breakdown in the enteric immune system and epithelial barrier function accounts for the systemic manifestations in *C. rodentium* wild-type-infected animals, as determined by changes in weight. In contrast to results with wild-type-infected mice, EID3 was found to poorly colonize organ cultures obtained from mesenteric lymph nodes, liver, or spleen, despite similar colon colonization counts on days 2 and 8 for wild-type and *lifA/efa1*-mutant *C. rodentium* strains.

Regardless of the enteric pathogen used in this study, all animals developed markedly increased epithelial cell regenerative scores during the 3-week infection. Unexpectedly, loss of goblet cells and massive crypt cell proliferation were observed only in mice infected with wild-type *C. rodentium*. It appears that lymphostatin/Efa1 elicits a direct or indirect effect on undifferentiated epithelial cells located on the bottom of colonic crypts. The mechanism by which lymphostatin/Efa1 mediates this effect is currently unclear, with three possible explanations for the phenomenon. First, infection with *C. rodentium* has been shown to induce a fourfold increase in total cellular β-catenin protein concentrations by day 12 in vivo (36). An increase in cellular β-catenin was accompanied by an increase in nuclear β-catenin concentrations, and elevated levels preceded crypt length elongation by about 2 days. The same study revealed that cellular concentrations of cyclin D1 and c-Myc, two proteins maintaining proliferation status, were increased. Without significant differences in bacterial adhesion in vitro and in vivo between results with wild-type and *lifA/efa1*-mutant *C. rodentium*, it is attractive to speculate that lymphostatin/Efa1 has a direct or indirect effect on epithelial cell proliferation mediated through the nuclear translocation of β-catenin. Second, the possibility of an indirectly mediated increase in cell proliferation in response to lymphostatin/Efa1 might exist through an effect on a host factor, such as early growth response factor-1 (EGR-1). In vitro and in vivo experiments performed with *C. rodentium* lead to an increased transcription of EGR-1 with subsequent activation of the MEK/extracellular signal-regulated kinases (9), a signal transduction pathway critical for cell proliferation (23). This effect was dependent on an intact type III secretion mechanism, which was necessary for the full induction of EGR-1 expression. A third explanation is the fact that infection with *C. rodentium* leads to an increase in production of keratinocyte growth factor (16), which binds to its cognate receptor on epithelial cells, inducing cell proliferation (2).

In conclusion, we have shown that *lifA/efa1* plays a role in the systemic manifestations of enteric infection with *C. rodentium*. Further, *lifA/efa1* positively regulates epithelial cell proliferation, colonic inflammation, and the development of TMCH. *lifA/efa1* is the first gene outside the LEE island that plays a critical role in the pathogenesis of *C. rodentium* infection.

ACKNOWLEDGMENTS

J.-M.A.K. was supported by a grant from the American Digestive Health Foundation and by Public Health Service grants KO8 DK062899-02 and R24DK64399. M.S.D. and P.J.F. were funded by Public Health Service awards AI32074 and AI37606 from the National Institutes of Health.

REFERENCES

1. **Badea, L., S. Doughty, L. Nicholls, J. Sloan, R. M. Robins-Browne, and E. L. Hartland.** 2003. Contribution of Efa1/LifA to the adherence of enteropathogenic *Escherichia coli* to epithelial cells. Microb. Pathog. **34:**205–215.
2. **Bajaj-Elliott, M., R. Poulsom, S. L. Pender, N. C. Wathen, and T. T. MacDonald.** 1998. Interactions between stromal cell-derived keratinocyte growth factor and epithelial transforming growth factor in immune-mediated crypt cell hyperplasia. J. Clin. Investig. **102:**1473–1480.
3. **Busch, C., F. Hofmann, J. Selzer, S. Munro, D. Jeckel, and K. Aktories.** 1998. A common motif of eukaryotic glycosyltransferases is essential for the enzyme activity of large clostridial cytotoxins. J. Biol. Chem. **273:**19566–19572.
4. **Busch, C., K. Schömig, F. Hofmann, and K. Aktories.** 2000. Characterization of the catalytic domain of *Clostridium novyi* alpha-toxin. Infect. Immun. **68:**6378–6383.
5. **Celli, J., M. Olivier, and B. B. Finlay.** 2001. Enteropathogenic *Escherichia coli* mediates antiphagocytosis through the inhibition of PI 3-kinase-dependent pathways. EMBO J. **20:**1245–1258.
6. **Czerucka, D., S. Dahan, B. Mograbi, B. Rossi, and P. Rampal.** 2001. Implication of mitogen-activated protein kinases in T84 cell responses to enteropathogenic *Escherichia coli* infection. Infect. Immun. **69:**1298–1305.
7. **Datsenko, K. A., and B. L. Wanner.** 2000. One-step inactivation of chromosomal genes in *Escherichia coli* K-12 using PCR products. Proc. Natl. Acad. Sci. USA **97:**6640–6645.
8. **Davidson, D. J., A. J. Currie, G. S. Reid, D. M. Bowdish, K. L. MacDonald, R. C. Ma, R. E. Hancock, and D. P. Speert.** 2004. The cationic antimicrobial peptide LL-37 modulates dendritic cell differentiation and dendritic cell-induced T cell polarization. J. Immunol. **172:**1146–1156.
9. **de Grado, M., C. M. Rosenberger, A. Gauthier, B. A. Vallance, and B. B. Finlay.** 2001. Enteropathogenic *Escherichia coli* infection induces expression of the early growth response factor by activating mitogen-activated protein kinase cascades in epithelial cells. Infect. Immun. **69:**6217–6224.
10. **Deng, W., Y. Li, B. A. Vallance, and B. B. Finlay.** 2001. Locus of enterocyte effacement from *Citrobacter rodentium*: sequence analysis and evidence for

horizontal transfer among attaching and effacing pathogens. Infect. Immun. **69:**6323–6335.
11. **Deng, W., B. A. Vallance, Y. Li, J. L. Puente, and B. B. Finlay.** 2003. *Citrobacter rodentium* translocated intimin receptor (Tir) is an essential virulence factor needed for actin condensation, intestinal colonization and colonic hyperplasia in mice. Mol. Microbiol. **48:**95–115.
12. **Donnenberg, M. S., C. O. Tacket, G. Losonsky, G. Frankel, J. P. Nataro, G. Dougan, and M. M. Levine.** 1998. Effect of prior experimental human enteropathogenic *Escherichia coli* infection on illness following homologous and heterologous rechallenge. Infect. Immun. **66:**52–58.
13. **Donnenberg, M. S., S. Tzipori, M. L. McKee, A. D. O'Brien, J. Alroy, and J. B. Kaper.** 1993. The role of the *eae* gene of enterohemorrhagic *Escherichia coli* in intimate attachment in vitro and in a porcine model. J. Clin. Investig. **92:**1418–1424.
14. **Gruenheid, S., I. Sekirov, N. A. Thomas, W. Deng, P. O'Donnell, D. Goode, Y. Li, E. A. Frey, N. F. Brown, P. Metalnikov, T. Pawson, K. Ashman, and B. B. Finlay.** 2004. Identification and characterization of NleA, a non-LEE-encoded type III translocated virulence factor of enterohaemorrhagic *Escherichia coli* O157:H7. Mol. Microbiol. **51:**1233–1249.
15. **Higgins, L. M., G. Frankel, I. Connerton, N. S. Goncalves, G. Dougan, and T. T. MacDonald.** 1999. Role of bacterial intimin in colonic hyperplasia and inflammation. Science **285:**588–591.
16. **Higgins, L. M., G. Frankel, G. Douce, G. Dougan, and T. T. MacDonald.** 1999. *Citrobacter rodentium* infection in mice elicits a mucosal Th1 cytokine response and lesions similar to those in murine inflammatory bowel disease. Infect. Immun. **67:**3031–3039.
17. **Just, I., J. Selzer, F. Hofmann, G. A. Green, and K. Aktories.** 1996. Inactivation of Ras by *Clostridium sordellii* lethal toxin-catalyzed glucosylation. J. Biol. Chem. **271:**10149–10153.
18. **Just, I., J. Selzer, M. Wilm, C. von Eichel-Streiber, M. Mann, and K. Aktories.** 1995. Glucosylation of Rho proteins by *Clostridium difficile* toxin B. Nature **375:**500–503.
19. **Kenny, B., L. C. Lai, B. B. Finlay, and M. S. Donnenberg.** 1996. EspA, a protein secreted by enteropathogenic *Escherichia coli*, is required to induce signals in epithelial cells. Mol. Microbiol. **20:**313–323.
20. **Klapproth, J. M., M. S. Donnenberg, J. M. Abraham, H. L. Mobley, and S. P. James.** 1995. Products of enteropathogenic *Escherichia coli* inhibit lymphocyte activation and lymphokine production. Infect. Immun. **63:**2248–2254.
21. **Klapproth, J. M., I. C. Scaletsky, B. P. McNamara, L. C. Lai, C. Malstrom, S. P. James, and M. S. Donnenberg.** 2000. A large toxin from pathogenic *Escherichia coli* strains that inhibits lymphocyte activation. Infect. Immun. **68:**2148–2155.
22. **Kresse, A. U., M. Rohde, and C. A. Guzman.** 1999. The EspD protein of enterohemorrhagic *Escherichia coli* is required for the formation of bacterial surface appendages and is incorporated in the cytoplasmic membranes of target cells. Infect. Immun. **67:**4834–4842.
22a. **Levine, M. M., E. J. Bergquist, D. R. Nalin, D. H. Waterman, R. B. Hornick, C. R. Young, S. Sotman, and B. Rowe.** 1978. *Escherichia coli* strains that cause diarrhea but do not produce heat-labile or heat-stable enterotoxins and are non-invasive. Lancet **i:**1119–1122.
23. **Loda, M., P. Capodieci, R. Mishra, H. Yao, C. Corless, W. Grigioni, Y. Wang, C. Magi-Galluzzi, and P. J. Stork.** 1996. Expression of mitogen-activated protein kinase phosphatase-1 in the early phases of human epithelial carcinogenesis. Am. J. Pathol. **149:**1553–1564.
24. **Luperchio, S. A., J. V. Newman, C. A. Dangler, M. D. Schrenzel, D. J. Brenner, A. G. Steigerwalt, and D. B. Schauer.** 2000. *Citrobacter rodentium*, the causative agent of transmissible murine colonic hyperplasia, exhibits clonality: synonymy of *C. rodentium* and mouse-pathogenic *Escherichia coli*. J. Clin. Microbiol. **38:**4343–4350.
25. **Mack, D. R., S. Michail, S. Wei, L. McDougall, and M. A. Hollingsworth.** 1999. Probiotics inhibit enteropathogenic *E. coli* adherence in vitro by inducing intestinal mucin gene expression. Am. J. Physiol. **276:**G941–G950.
26. **McDaniel, T. K., and J. B. Kaper.** 1997. A cloned pathogenicity island from enteropathogenic *Escherichia coli* confers the attaching and effacing phenotype on *E. coli* K-12. Mol. Microbiol. **23:**399–407.
27. **Moon, H. W., S. C. Whipp, R. A. Argenzio, M. M. Levine, and R. A. Giannella.** 1983. Attaching and effacing activities of rabbit and human enteropathogenic *Escherichia coli* in pig and rabbit intestines. Infect. Immun. **41:**1340–1351.
28. **Moyenuddin, M., and K. M. Rahman.** 1985. Enteropathogenic *Escherichia coli* diarrhea in hospitalized children in Bangladesh. J. Clin. Microbiol. **22:**838–840.
29. **Mundy, R., D. Pickard, R. K. Wilson, C. P. Simmons, G. Dougan, and G. Frankel.** 2003. Identification of a novel type IV pilus gene cluster required for gastrointestinal colonization of *Citrobacter rodentium*. Mol. Microbiol. **48:**795–809.
30. **Newman, J. V., B. A. Zabel, S. S. Jha, and D. B. Schauer.** 1999. Citrobacter rodentium *espB* is necessary for signal transduction and for infection of laboratory mice. Infect. Immun. **67:**6019–6025.
31. **Nicholls, L., T. H. Grant, and R. M. Robins-Browne.** 2000. Identification of a novel genetic locus that is required for in vitro adhesion of a clinical isolate of enterohaemorrhagic *Escherichia coli* to epithelial cells. Mol. Microbiol. **35:**275–288.
32. **Posfai, G., M. Koob, Z. Hradecna, N. Hasan, M. Filutowicz, and W. Szybalski.** 1994. In vivo excision and amplification of large segments of the *Escherichia coli* genome. Nucleic Acids Res. **22:**2392–2398.
32a. **Posfai G., M. D. Koob, H. A. Kirkpatrick, and F. R. Blattner.** 1997. A *Salmonella typhimurium* virulence protein is similar to a *Yersinia enterocolitica* invasion protein and a bacteriophage Lambda outer membrane protein. J. Bacteriol. **173:**86–83.
33. **Read, T. D., G. S. Myers, R. C. Brunham, W. C. Nelson, I. T. Paulsen, J. Heidelberg, E. Holtzapple, H. Khouri, N. B. Federova, H. A. Carty, L. A. Umayam, D. H. Haft, J. Peterson, M. J. Beanan, O. White, S. L. Salzberg, R. C. Hsia, G. McClarty, R. G. Rank, P. M. Bavoil, and C. M. Fraser.** 2003. Genome sequence of *Chlamydophila caviae* (*Chlamydia psittaci* GPIC): examining the role of niche-specific genes in the evolution of the *Chlamydiaceae*. Nucleic Acids Res. **31:**2134–2147.
34. **Schauer, D. B., and S. Falkow.** 1993. Attaching and effacing locus of a *Citrobacter freundii* biotype that causes transmissible murine colonic hyperplasia. Infect. Immun. **61:**2486–2492.
35. **Schmidt, H., and H. Karch.** 1996. Enterohemolytic phenotypes and genotypes of Shiga toxin-producing *Escherichia coli* O111 strains from patients with diarrhea and hemolytic-uremic syndrome. J. Clin. Microbiol. **34:**2364–2367.
36. **Sellin, J. H., S. Umar, J. Xiao, and A. P. Morris.** 2001. Increased beta-catenin expression and nuclear translocation accompany cellular hyperproliferation in vivo. Cancer Res. **61:**2899–2906.
37. **Shao, F., P. M. Merritt, Z. Bao, R. W. Innes, and J. E. Dixon.** 2002. A *Yersinia* effector and a *Pseudomonas* avirulence protein define a family of cysteine proteases functioning in bacterial pathogenesis. Cell **109:**575–588.
38. **Shao, F., P. O. Vacratsis, Z. Bao, K. E. Bowers, C. A. Fierke, and J. E. Dixon.** 2003. Biochemical characterization of the *Yersinia* YopT protease: cleavage site and recognition elements in Rho GTPases. Proc. Natl. Acad. Sci. USA **100:**904–909.
39. **Stevens, M. P., P. M. van Diemen, G. Frankel, A. D. Phillips, and T. S. Wallis.** 2002. Efa1 influences colonization of the bovine intestine by Shiga toxin-producing *Escherichia coli* serotypes O5 and O111. Infect. Immun. **70:**5158–5166.
40. **Stone, K. D., H. Z. Zhang, L. K. Carlson, and M. S. Donnenberg.** 1996. A cluster of fourteen genes from enteropathogenic *Escherichia coli* is sufficient for the biogenesis of a type IV pilus. Mol. Microbiol. **20:**325–337.
41. **Tani, K., W. J. Murphy, O. Chertov, R. Salcedo, C. Y. Koh, I. Utsunomiya, S. Funakoshi, O. Asai, S. H. Herrmann, J. M. Wang, L. W. Kwak, and J. J. Oppenheim.** 2000. Defensins act as potent adjuvants that promote cellular and humoral immune responses in mice to a lymphoma idiotype and carrier antigens. Int. Immunol. **12:**691–700.
42. **Tatsuno, I., M. Horie, H. Abe, T. Miki, K. Makino, H. Shinagawa, H. Taguchi, S. Kamiya, T. Hayashi, and C. Sasakawa.** 2001. *toxB* gene on pO157 of enterohemorrhagic *Escherichia coli* O157:H7 is required for full epithelial cell adherence phenotype. Infect. Immun. **69:**6660–6669.
43. **Yang, D., O. Chertov, S. N. Bykovskaia, Q. Chen, M. J. Buffo, J. Shogan, M. Anderson, J. M. Schroder, J. M. Wang, O. M. Howard, and J. J. Oppenheim.** 1999. Beta-defensins: linking innate and adaptive immunity through dendritic and T cell CCR6. Science **286:**525–528.
44. **Zhu, C., T. S. Agin, S. J. Elliott, L. A. Johnson, T. E. Thate, J. B. Kaper, and E. C. Boedeker.** 2001. Complete nucleotide sequence and analysis of the locus of enterocyte effacement from rabbit diarrheagenic *Escherichia coli* RDEC-1. Infect. Immun. **69:**2107–2115.

Editor: J. B. Bliska

INFECTION AND IMMUNITY, May 2005, p. 3196 Vol. 73, No. 5
0019-9567/05/$08.00+0 doi:10.1128/IAI.73.5.3196.2005

ERRATUM

Citrobacter rodentium lifA/efa1 Is Essential for Colonic Colonization and Crypt Cell Hyperplasia In Vivo

Jan-Michael A. Klapproth, Maiko Sasaki, Melanie Sherman, Brian Babbin, Michael S. Donnenberg, Paula J. Fernandes, Isabel C. A. Scaletsky, Daniel Kalman, Asma Nusrat, and Ifor R. Williams

Division of Digestive Diseases and Department of Pathology, Emory University, Atlanta, Georgia; Division of Infectious Diseases, University of Maryland, Baltimore, Maryland; and Departamento de Microbiologia, Imunologia, e Parasitologia, Universidade Federal de São Paulo, São Paulo, Brazil

Volume 73, no. 3, p. 1441–1451, 2005. Page 1447: Figure 4 should appear as shown below.